Supporting Information

A universal route to fabricate hierarchically ordered macro-/mesoporous oxides with enhanced intrinsic activity

Ying Xin,[a] Pin Jiang,[a] Mingqiang Yu,[a] Huachun Gu,[a] Qian Li,[a] Zhaoliang Zhang*[a,b]

[a] School of Chemistry and Chemical Engineering, University of Jinan, 336 Nanxinzhuangxi Road, Jinan 250022, China

[b] State Key Laboratory of Materials-Oriented Chemical Engineering, Nanjing University of Technology, Nanjing, 210009, China

Contents:

1. Tables

Table S1 Elemental compositions of hierarchically ordered macro-/mesoporous Ce_aTiO_x.

Sample	Ce/Ti atomic ratio [a]	Ce/Ti atomic ratio [b]
$Ce_{0.2}TiO_x$	0.2	0.21
$Ce_{0.3}TiO_x$	0.3	0.33
$Ce_{0.5}TiO_x$	0.5	0.51
$Ce_{0.7}TiO_x$	0.7	0.73
$Ce_{1.0}TiO_x$	1.0	1.06

[a]: The data are the nominal Ce/Ti atomic ratios in Ce–Ti mixed oxides.

[b]: The data were obtained by quantitatively analyzing distribution mapping results.

Table S2 BET surface areas, pore volumes and average pore sizes of the hierarchically ordered macro-/mesoporous Ce_aTiO_x.

Sample	BET surface area [m^2 g^{-1}]			Pore volume [cm^3 g^{-1}]			Average pore size [nm]	
	Macropore (> 50 nm)	Mesopore (≤ 50 nm)	Total	Macropore (> 50 nm)	Mesopore (≤ 50 nm)	Total	Macropore [a] (> 50 nm)	Mesopore (≤ 50 nm)
$Ce_{0.2}TiO_x$	1.18	55.15	56	0.0282	0.1112	0.140	195	8.2
$Ce_{0.3}TiO_x$	2.25	44.99	46	0.0484	0.0842	0.133	197	11.2
$Ce_{0.5}TiO_x$	1.64	40.88	43	0.0341	0.0640	0.098	197	9.5
$Ce_{0.7}TiO_x$	1.38	26.58	28	0.033	0.0622	0.095	194	15.1
$Ce_{1.0}TiO_x$	1.38	25.72	27	0.031	0.0543	0.085	197	17.0

[a]: Estimated according to the SEM and TEM images.

Table S3. BET surface areas, pore volumes, and average pore sizes of the Ce_aTiO_x–n.

Sample	BET surface area [m^2 g^{-1}]	Pore volume [cm^3 g^{-1}]	Average pore size [nm]
$Ce_{0.2}TiO_x$–n	120[a]	0.337	9.3
$Ce_{0.3}TiO_x$–n	122 [a]	0.424	14.3
$Ce_{0.5}TiO_x$–n	79 [a]	0.214	13.7
$Ce_{0.7}TiO_x$–n	61	0.146	7.9
$Ce_{1.0}TiO_x$–n	25	0.078	12.0

[a]: From Ref. S1.

2. Figures

Figure S1

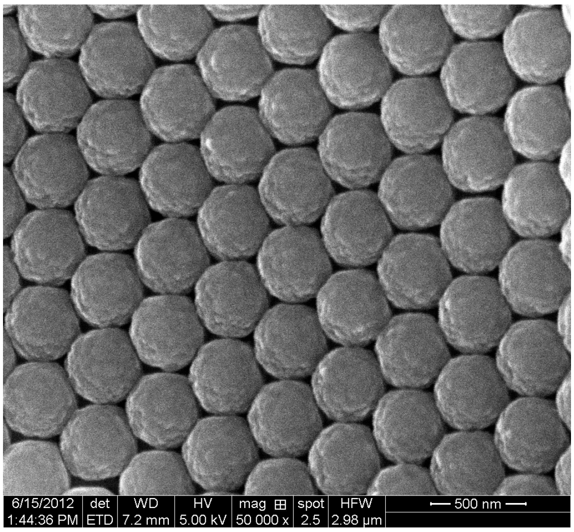

Fig. S1 SEM image of the colloidal crystal template assembled by 389 nm PMMA spheres.

Figure S2

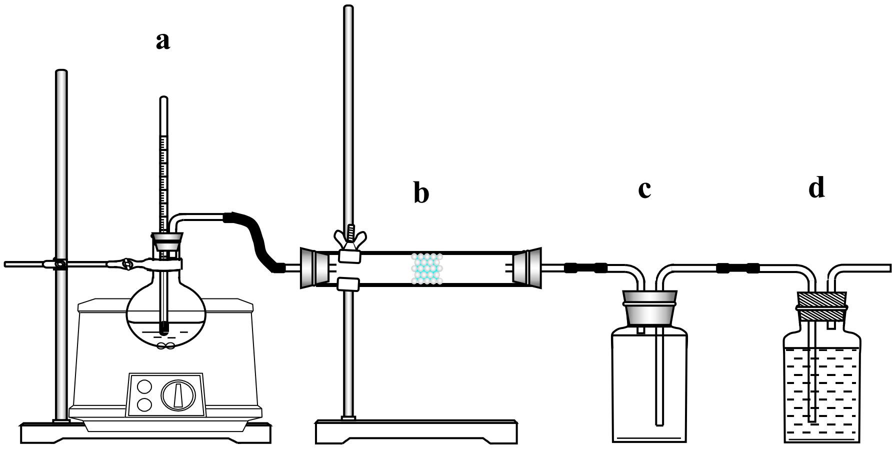

Fig. S2 Schematic illustration of a self-made wet ammonia gas infiltration-precipitation device: (a) wet ammonia gas generator; (b) infiltrated-precipitation device; (c) anti-reverse suction flask; (d) scrubbing bottle.

Figure S3

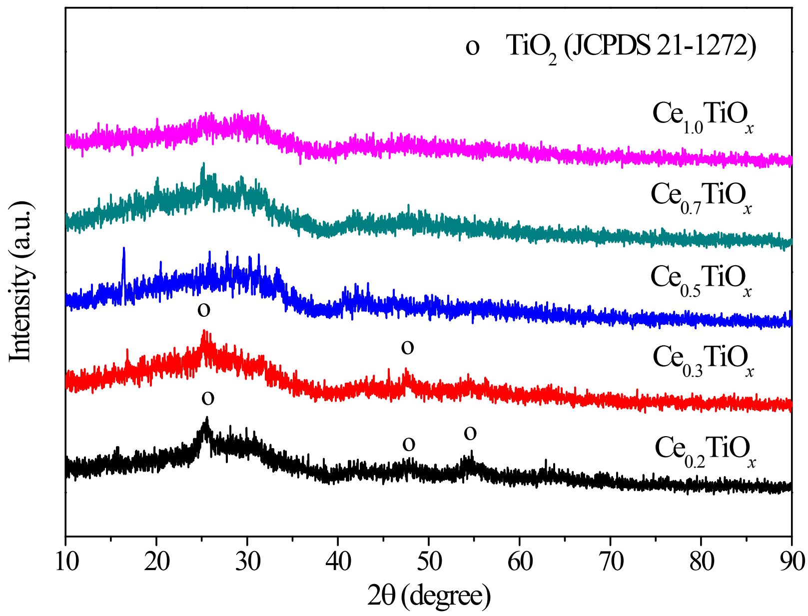

Fig. S3 XRD patterns of the as-fabricated hierarchical macro-/mesoporous Ce_aTiO_x.

Figure S4

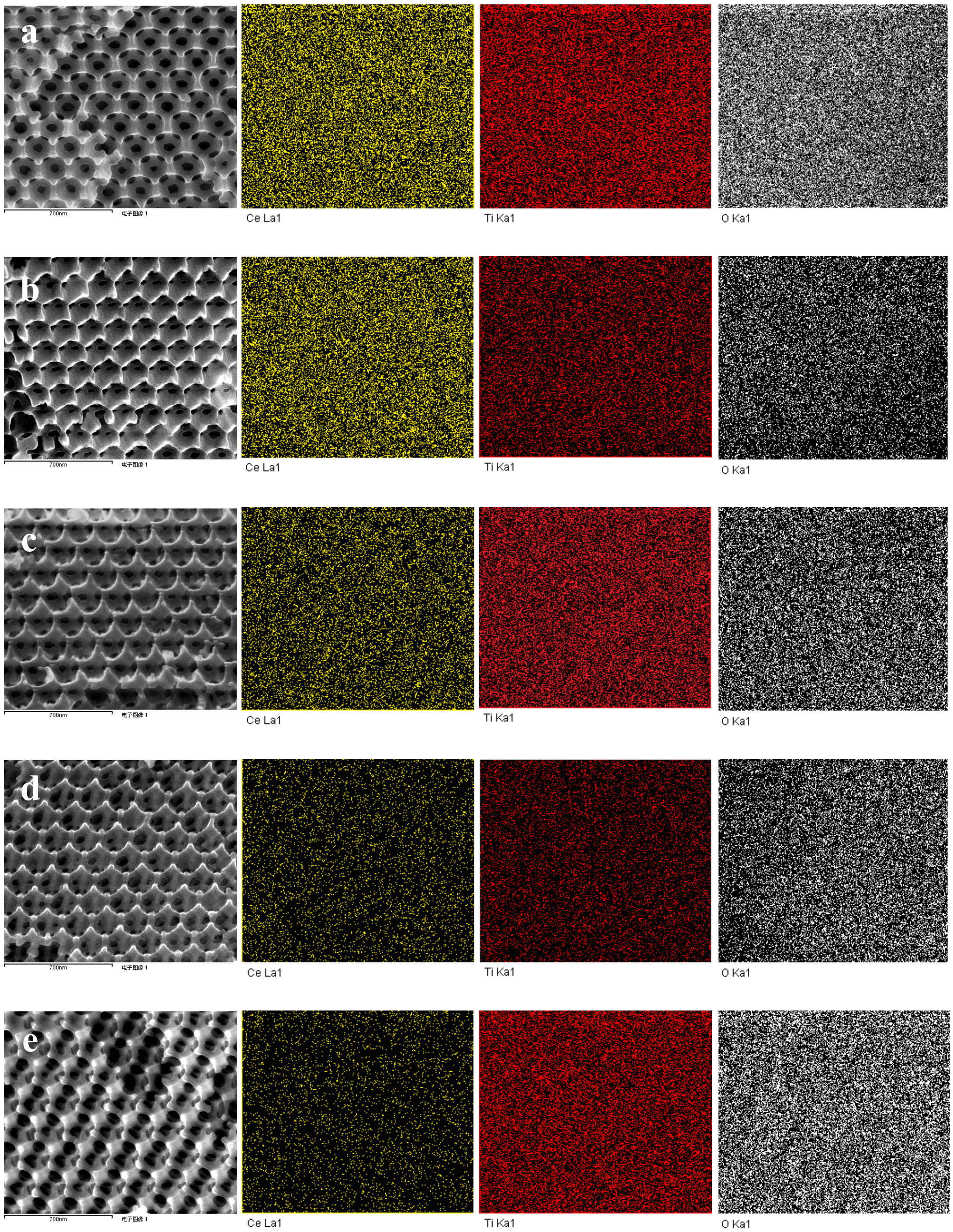

Fig. S4 SEM images and the corresponding distribution maps of Ce, Ti and O elements for the hierarchical macro-/mesoporous Ce_aTiO_x: (a) $Ce_{0.2}TiO_x$; (b) $Ce_{0.3}TiO_x$; (c) $Ce_{0.5}TiO_x$; (d) $Ce_{0.7}TiO_x$; (e) $Ce_{1.0}TiO_x$.

Figure S5

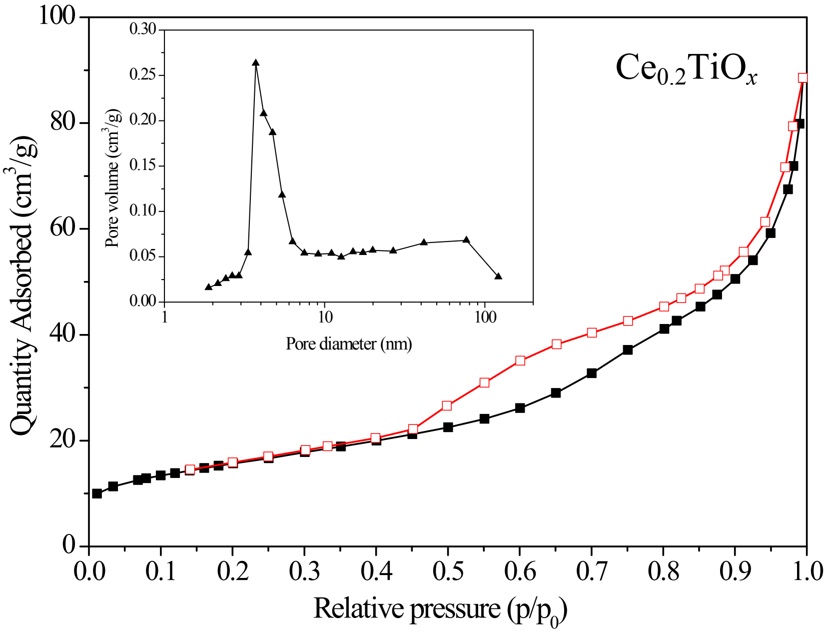

Ce0.2TiOx
Quantity Adsorbed (cm3/g)
Relative pressure (p/p0)
Pore volume (cm3/g)
Pore diameter (nm)

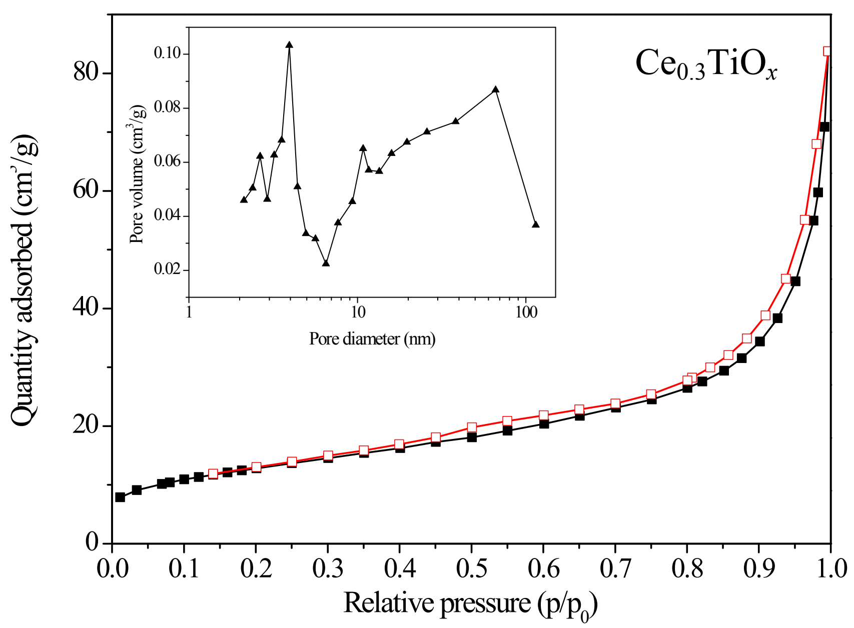

Ce0.3TiOx
Quantity adsorbed (cm3/g)
Relative pressure (p/p0)
Pore volume (cm3/g)
Pore diameter (nm)

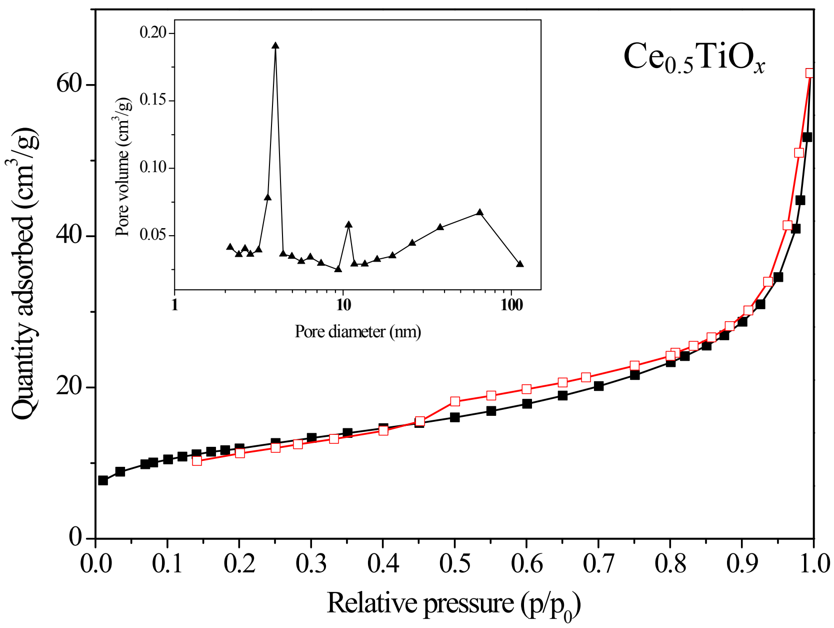
Ce$_{0.5}$TiO$_x$
Quantity adsorbed (cm^3/g)
Relative pressure (p/p$_0$)
Pore volume (cm^3/g)
Pore diameter (nm)

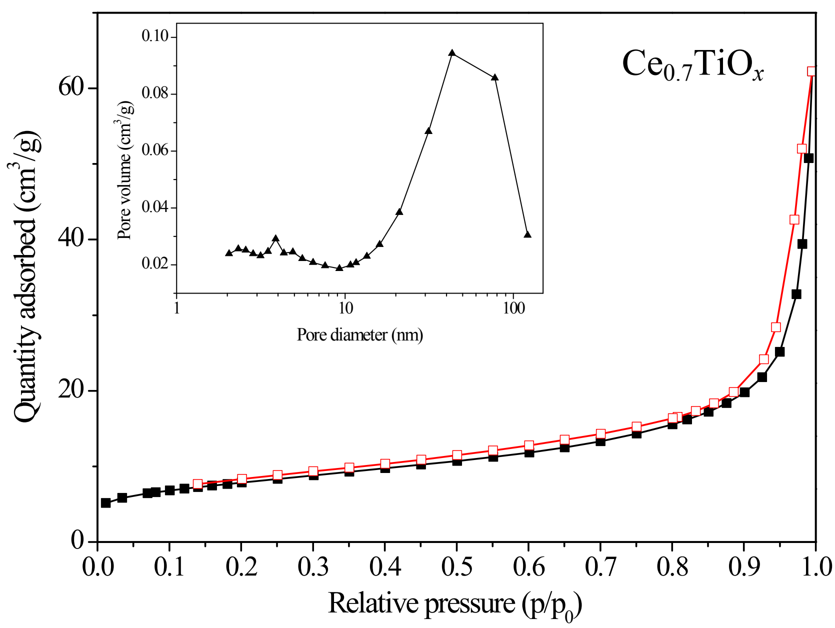
Ce$_{0.7}$TiO$_x$
Quantity adsorbed (cm^3/g)
Relative pressure (p/p$_0$)
Pore volume (cm^3/g)
Pore diameter (nm)

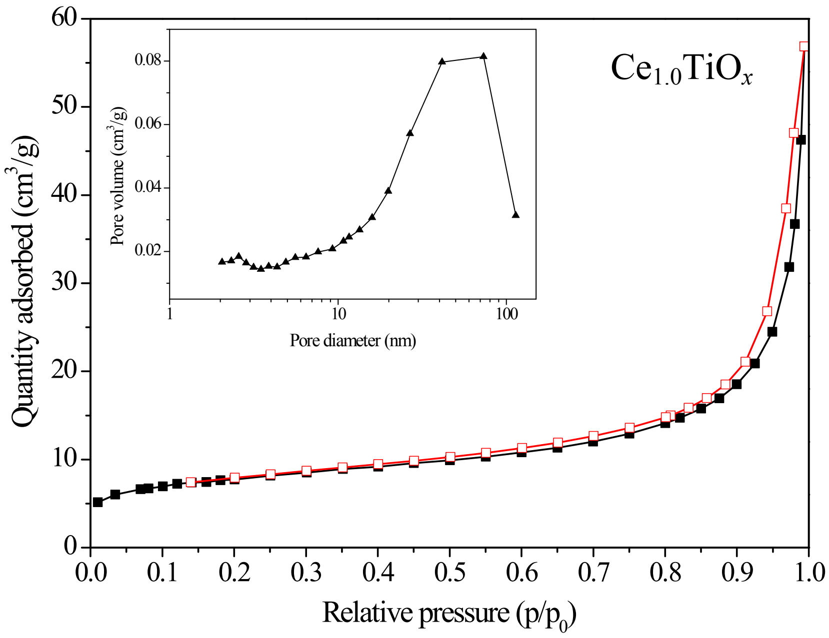

Fig. S5 N_2 adsorption/desorption isotherms and pore size distribution curves (insets) for Ce_aTiO_x.

Figure S6

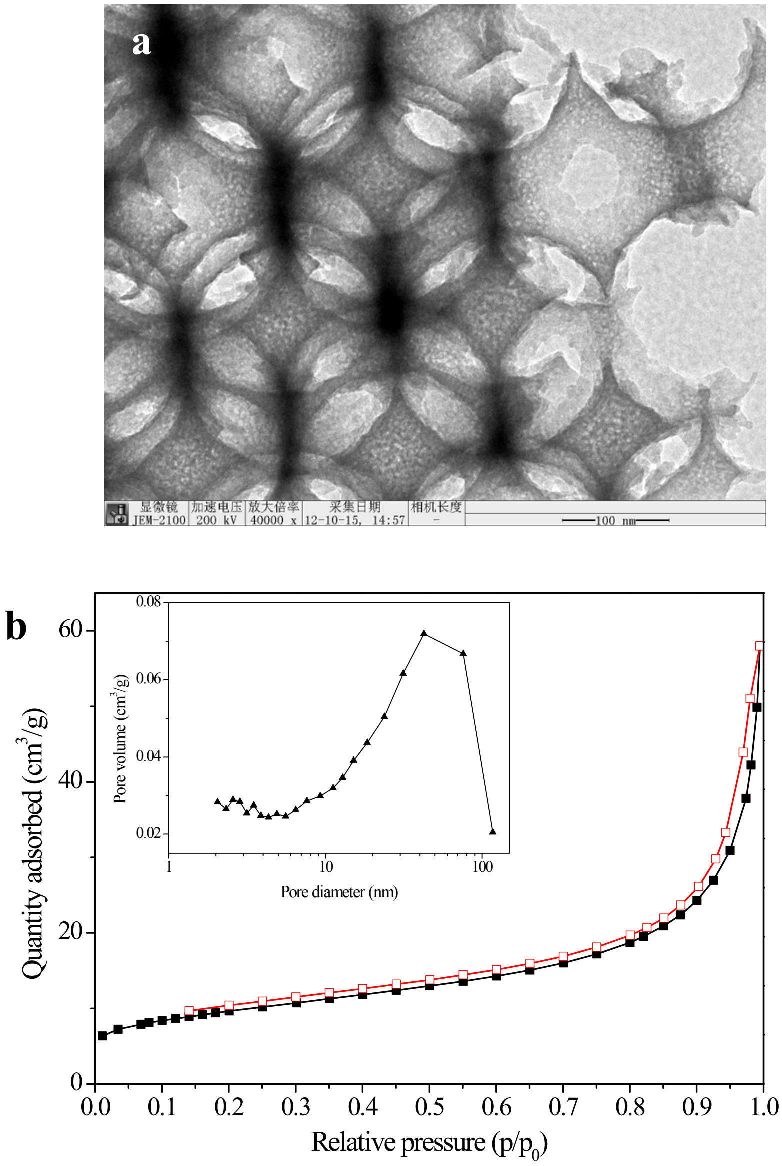

Fig. S6 (a) TEM image and (b) N_2 adsorption/desorption isotherms and pore size distribution curve (inset) of $Ce_{0.3}TiO_x$–air.

Figure S7

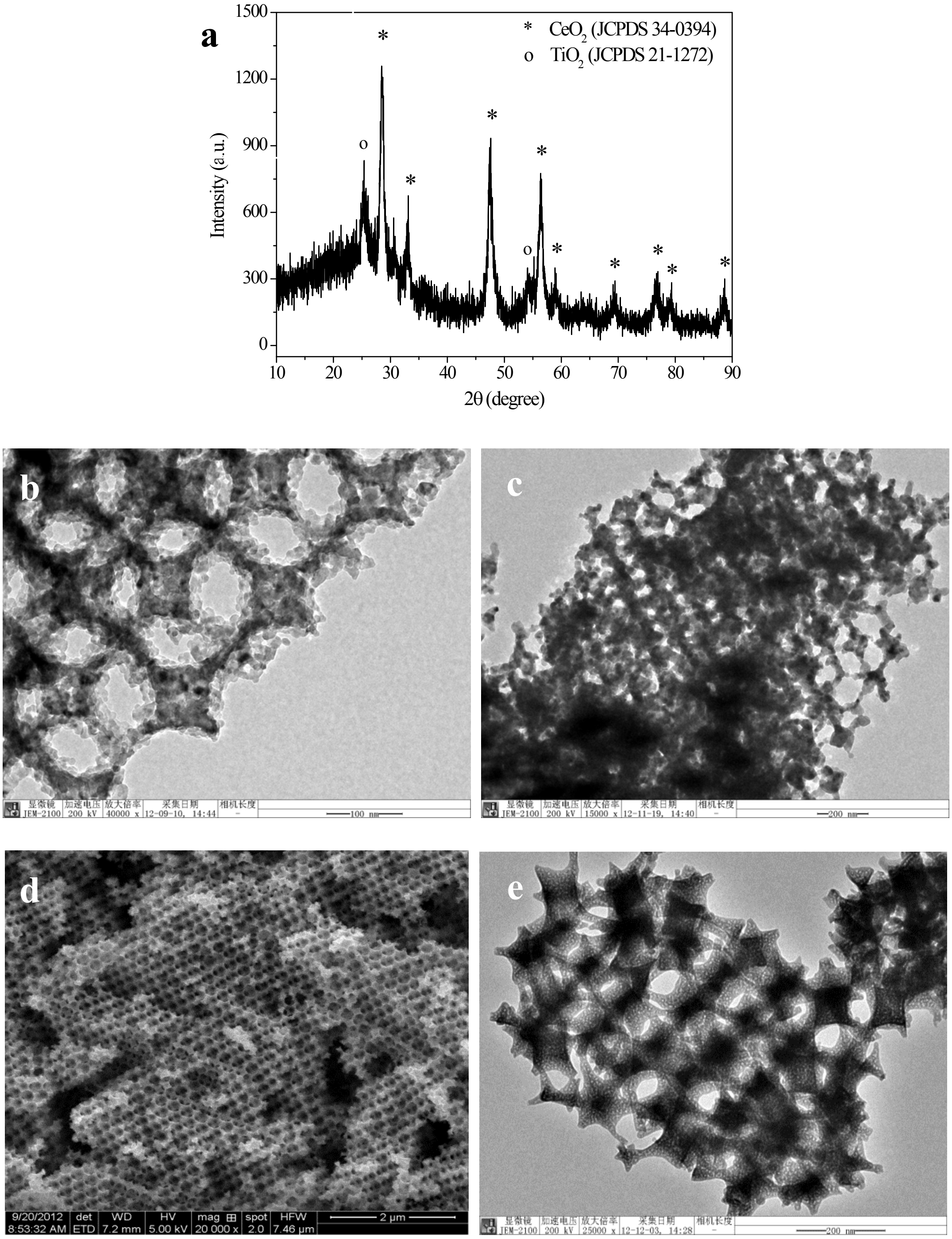
a
1500
1200
900
600
300
0
Intensity (a.u.)
10 20 30 40 50 60 70 80 90
2θ (degree)
* CeO_2 (JCPDS 34-0394)
o TiO_2 (JCPDS 21-1272)
b
显微镜 加速电压 放大倍率 采集日期 相机长度
JEM-2100 200 kV 40000 x 12-09-10, 14:44
100 nm
c
显微镜 加速电压 放大倍率 采集日期 相机长度
JEM-2100 200 kV 15000 x 12-11-19, 14:40
200 nm
d
9/20/2012 det WD HV mag spot HFW
8:53:32 AM ETD 7.2 mm 5.00 kV 20 000 x 2.0 7.46 μm
2 μm
e
显微镜 加速电压 放大倍率 采集日期 相机长度
JEM-2100 200 kV 25000 x 12-12-03, 14:28
200 nm

Fig. S7 (a) XRD pattern and (b) TEM image of $Ce_{0.3}TiO_x$–550, (c) TEM image of $Ce_{0.3}TiO_x$–650, (d) SEM and (e) TEM images of $Ce_{1.0}TiO_x$ after a mild pressing and grinding.

Figure S8

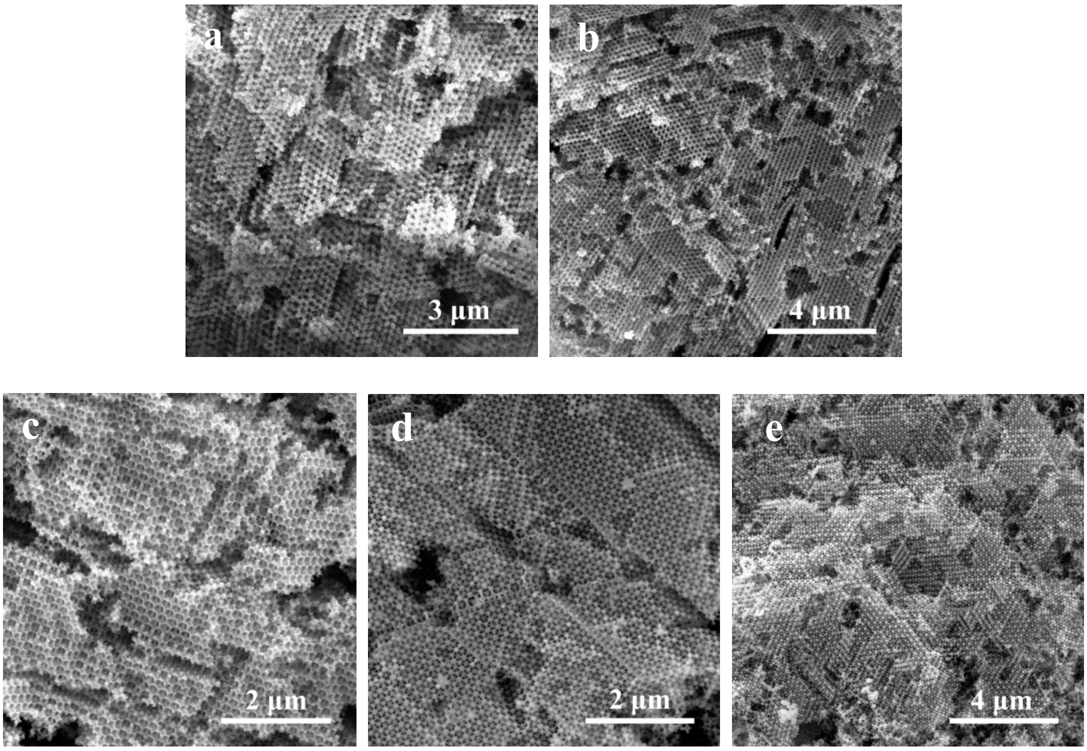

Fig. S8 SEM images of the hierarchically macro-/mesoporous Ce_aTiO_x after SCR reactions: (a) $Ce_{0.2}TiO_x$; (b) $Ce_{0.3}TiO_x$; (c) $Ce_{0.5}TiO_x$; (d) $Ce_{0.7}TiO_x$; (e) $Ce_{1.0}TiO_x$.

Figure S9

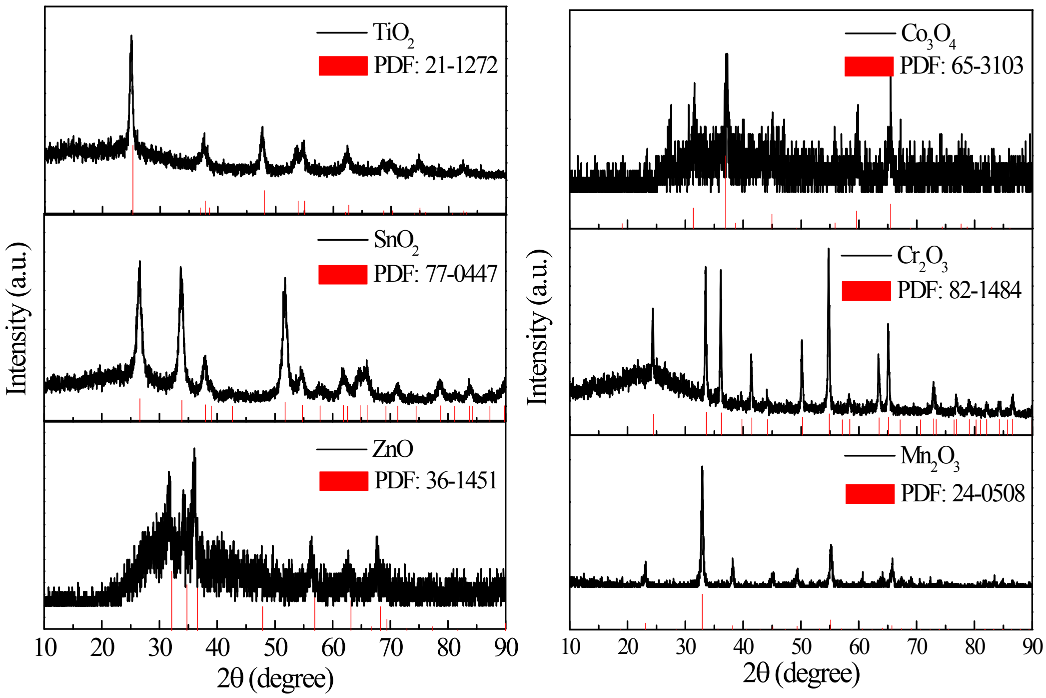

Fig. S9 XRD patterns of the hierarchical macro-/mesoporous unitary oxides.

Figure S10

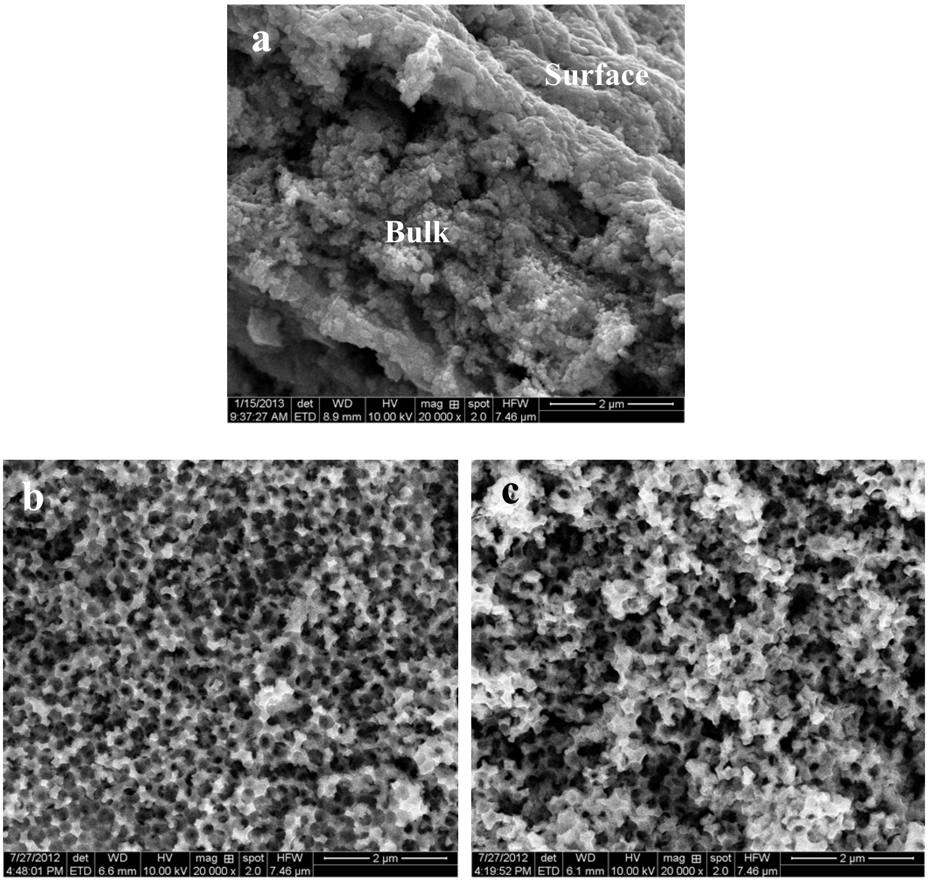

Fig. S10 SEM images of Mn_2O_3 synthesized using pure ammonia gas (a), $Ce_{0.3}TiO_x$ synthesized using ammonia water (b) and $Ce_{0.3}TiO_x$ synthesized without using wet ammonia gas infiltration-precipitation route (c).

3. References

[S1] P. Li, Y. Xin, Q. Li, Z. P. Wang, Z. L. Zhang and L. R. Zheng, *Environ. Sci. Technol.*, 2012, **46**, 9600–9605.